JOURNAL OF INFORMATION SCIENCE AND ENGINEERING 21, 1139-1156 (2005)

Fuzzy Hysteresis Control and Parameter Optimization of a Shunt Active Power Filter*

B. MAZARI AND F. MEKRI
Electrical Engineering Department
University of Sciences and Technology of Oran Mohamed-Boudiaf
BP 1505 El Mnaouer Oran-Algeria
E-mail: {mazari_dz; mekri_dz}@yahoo.fr

This paper presents the optimization of shunt active power filter parameters based on fuzzy logic control. The current active filter control is based on constant, fuzzy hysteresis band techniques, which are employed to derive the switching signals and also to choose the optimal value of the decoupling inductance. The DC voltage controller optimizes the energy storage of the DC capacitor, where proportional integral and fuzzy logic controllers are employed. Simulation results, obtaining using MATLAB/SIMULINK under several loads configurations, are presented and discussed. They show the effectiveness of fuzzy logic controllers in optimizing the PWM technique and the values of the passive parameters of the active filter.

Keywords: active power filter (APF), fuzzy logic control, optimization, harmonics, PWM techniques

1. INTRODUCTION

The wide use of non-linear loads, such as with static power converters, is responsible for harmonic pollution problems. These loads draw non-sinusoidal currents that cause harmonic voltage drops across the network impedance, resulting in distorted voltages. Harmonic current pollution also has serious consequences such as increased power system losses, quick aging of materials, excessive heating in rotating machinery, and significant interference with communication circuits.

To avoid these undesirable effects, traditional solutions using passive LC filters have been used, but they are ineffective due to their inability to adapt to network characteristic variation. Therefore, recent progress in switching devices has resulted in the formulation of several active filter topologies, not only for current or voltage compensation but also for voltage dips, flicker, imbalance or other kinds of disturbances [1, 4].

The shunt active power filter (APF), generally based on a voltage source inverter structure, seems to be an attractive solution to harmonic current pollution problems. It can be used to compensate unbalanced currents, current harmonics, and reactive power. The mains currents, obtained after compensation, are then sinusoidal and in phase with the supply voltages [5, 6].

Received January 2, 2004; revised March 17, 2004; accepted May 6, 2004.
Communicated by Chuen-Tsai Sun.
* This article was presented at the 36th University's Power Engineering Conference UPEC 2001, 12-14 September 2001, Swansea, U.K.

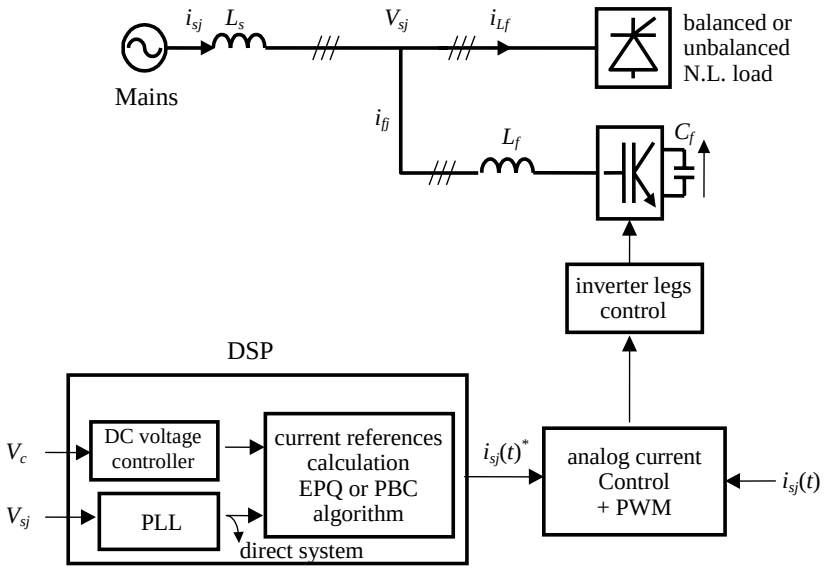

Fig. 1. Shunt active power filter.

The active power filter under study is presented in Fig. 1. The APF performance depends on the design of the power semiconductor device, on the modulation technique used to control the switches, on the design of the coupling elements. Connecting (L_f, C_f), respectively, on the AC and DC sides is one method used to determine active filter current references and the dynamics and robustness of current and DC voltage control loops [7]. Selective harmonics compensation can be used to meet standards and reduce the power rating of the APF as explained in [8].

In this paper, global current harmonics compensation is studied. To compensate harmonics and fundamental reactive power, two equivalent current control methods can be considered, according to whether the regulated variables are the line currents (i_s) or the active power filter currents (i_f). Our algorithm focuses on directly calculating and controlling the mains currents. The objective is to get sinusoidal line currents in phase with the supply voltages at the common coupling point. The standard "instantaneous power theory" or "p-q theory" are used to determine the current references [9]. The supply voltages at the common coupling point are considered to be sinusoidal and balanced. The aim of our work is to optimize the PWM technique using fuzzy logic controllers and the values of the passive parameters of the active filter using appropriate robust current and voltage controllers.

Optimal choices of the values of the decoupling inductance, L_f, and the capacitance C_f, of the DC capacitor will reduce the total harmonic distortion (THD) of the source current and the DC voltage variation under transients.

Among the various PWM techniques, the hysteresis band current control PWM is popularly used because of its simplicity of implementation. This technique does not need any information about the system parameters but has the disadvantage of uncontrolled frequency. As a result, the switching losses are increased and current sources contain

excess ripples [10]. The current controller performance can be improved by using the adaptive control system theory [11].

A new technique, based on the same concept, but with the hysteresis band implemented with fuzzy logic, is proposed to optimize the PWM performance. This approach permits us to define a systematic for computing a look-up control using the instantaneous supply voltage and mains current reference slop as input variables and the hysteresis band as an output variable to maintain the modulation frequency quasi constant.

For the DC supply source of the three phase active filter, PI and fuzzy logic controllers are studied and compared here. This investigation shows that a trade-off must be found between the two criteria in order to limit the total harmonic distortion ratio of the source current or to minimize the settling time and DC capacitor variation under transient conditions [12]. An appropriate voltage controller must be synthesized to assure high dynamic performance with simplified design of the capacitor.

In the last section, simulation results will be presented and discussed. They will show the efficiency of the fuzzy logic controllers in optimizing the APF parameters and assuring good compensation characteristics for the APF under steady-state, transient, and load asymmetrical conditions.

2. DC CAPACITOR DESIGN AND VOLTAGE CONTROL

The tasks of the APF are as follows:

- to achieve a high power factor (PF) with a linear or non linear load connected on the dc side;
- to compensate the current harmonics, fundamental reactive power, and imbalance due to non-linear loads connected on the ac mains;
- to maintain a constant output voltage (V_c) across the DC capacitor, C_f, with low ripple;
- to respond quickly to load disturbances and assure robustness against uncertainties in component values and operating conditions.

2.1 Design of the DC Bus Capacitor

The DC bus capacitor must be designed to achieve two goals, i.e., to comply with the minimum ripple requirement of the dc bus voltage and to limit the DC bus voltage variation during load transients.

The main currents after compensation are in phase with the supply voltages and can be expressed as

$$i_{sj} = \sqrt{2}.I_s.\sin(\omega t - \frac{2\pi}{3}(j-1)), \quad j = 1, 2, 3. \tag{1}$$

The real power supplied from the mains is

$$p_s(t) = \sum_{j=1}^{3} v_{sj}(t).i_{sj}(t) = 3V_s.I_s = P_s. \tag{2}$$

The instantaneous power absorbed by a given non linear load is

$$p_L(t) = \sum_{j=1}^{3} v_{sj}(t).i_{Lj}(t) = P_L + \tilde{p}_L(t). \tag{3}$$

The instantaneous power injected by the active power filter is given by

$$p_f(t) = p_L(t) - P_s = P_L - P_s + \tilde{p}_L(t) = P_f + \tilde{p}_f(t) \tag{4}$$

with

$$P_f = P_L - P_s \quad \text{and} \quad \tilde{p}_f(t) = \tilde{p}_L(t). \tag{5}$$

The components P_f, P_L, P_s, and $\tilde{p}_f(t)$, $\tilde{p}_L(t)$ represent, respectively, the average DC and alternating parts of the instantaneous powers.

Eqs. (4) and (5) illustrate the power exchange between the active power filter, nonlinear load, and network under load transient conditions as shown in Fig. 2.

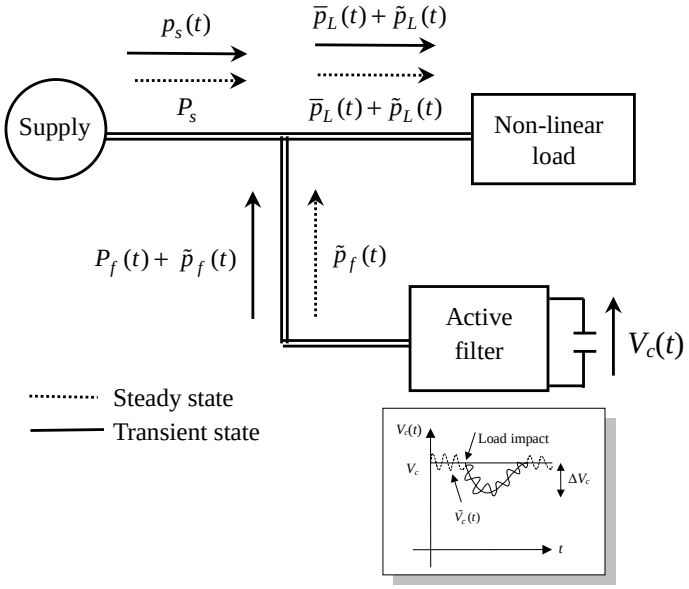

Fig. 2. Power exchange between network the APF and load.

We will consider later a three-phase rectifier as a polluting load.

The instantaneous power absorbed by the load is then given by

$$P_L(t) = 3V_s I_{L1} \cos(\phi) + \sum_{n=1}^{\infty} P_{3n}.\cos(3n\omega t - \varphi_{3n}). \tag{6}$$

Under steady-state operation, the APF does not exchange any power with the network. In this case, we have the following relations:

$$\tilde{p}_f(t) = \tilde{p}_L(t) = v_c(t) i_c(t). \tag{7}$$

The voltage ripple is then related to the capacitor current $i_c(t)$ by

$$\tilde{v}_c(t) = \frac{1}{C_f} \int_0^t i_c(t).dt = \frac{1}{C_f} \int_0^t \frac{\tilde{p}_L(t)}{V_c}.dt. \tag{8}$$

By assuming that the DC voltage ripple is essentially due to first harmonic currents, such as the 5th and 7th harmonic components, we obtain

$$\tilde{v}_c(t) = \frac{1}{C_f.V_c} \int_0^t \sum_{n=1}^{\infty} P_{6n}.\cos(6n\omega t - \varphi_{6n}).dt. \tag{9}$$

The DC voltage fluctuation is defined as

$$\varepsilon_v = \frac{\Delta V_c}{V_c} = \frac{V_{c\max} - V_{c\min}}{V_c}, \tag{10}$$

where V_{cmax}, V_{cmin}, and V_c represent, respectively, the maximum, minimum, and average values of the dc bus voltage. Thus, the value of the capacitor which will reduce the ripple voltage of the dc bus voltage is given by the following formula:

$$C_f = \frac{P_6}{3.\varepsilon_v.\omega.V_c^2} = \frac{V_s.\sqrt{I_5^2 + I_7^2 - 2.I_5.I_7.\cos\left[5\varphi_5 - 7\varphi_6\right]}}{\varepsilon_v.\omega.V_c^2}. \tag{11}$$

For our application, we tolerate a maximal voltage ripple of 2.5% to take into account the worst case under harmonics and excessive unbalanced conditions. The DC bus voltage is fixed at 700V, and the capacitor value is chosen equal to 1 mF.

Note that the modification of the C_f value does not considerably affect the magnitude of the voltage fluctuation. However, the choice of C_f can have serious effects on the DC voltage variation under transients. Thus, a compromise must be found between the C_f value and the performance of the DC capacitor voltage controller (including the time response and limitation of the deep or hump voltage under a sudden increase or decrease of the load).

2.2 DC Voltage Control

If switching losses are neglected, the real power absorbed by the APF can be expressed as

$$P_f = -\frac{1}{2} C_f \frac{dv_c^2(t)}{dt}. \tag{12}$$

If Laplace transformation is performed, the model for the real power analysis and the DC voltage control scheme can be easily deduced.

The aim of the synthesized voltage regulator is to adjust $v_c^2(t)$ to its reference value to reject the internal disturbance (dI) of the system due to the real power, P_L, and to assure good filtering of the external one (dE) due to the alternating power $\tilde{P}_L(t)$. To realize these objectives, proportional integral and fuzzy logic controllers will be considered and compared.

2.2.1 Integral proportional controller

The simplified functional scheme of the voltage control based on a PI regulator is presented in Fig. 3.

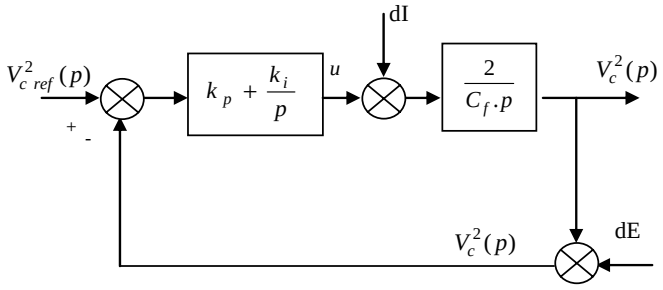

Fig. 3. Block diagram of the DC voltage control using a PI controller.

The required system natural frequency imposed by the voltage controller must be smaller than the minimum frequency of current compensation to be injected by the converter in order to avoid interaction between the voltage controller and harmonic current injection system.

The closed loop transfer function of DC voltage is given by

$$F(s) = \frac{\omega_c^2(1+\tau s)}{s^2 + 2\xi\omega_c s + \omega_c^2} \tag{13}$$

with $\tau = \frac{k_p}{k_i}$, $\tau_1 = \frac{1}{k_i}$ and $\omega_c = \sqrt{\frac{2}{C_f \tau_1}} = 2\pi f_o$.

Here, k_p and k_i are the regulator parameters. Note that the dynamic of regulation is imposed by the time constant, τ_1, through the choice of the cut-off frequency, f_o. This frequency will influence the performance of the PI regulator under transient load conditions, including the time response, t_r, DC voltage variations, ΔV_c, under a step change of the nonlinear load current, and the total harmonic ratio, THD, of the mains current [13]. A trade off must, consequently, is found between the two criteria in order to limit the THD of the source current or to minimize ΔV_c and t_r.

The total harmonic ratio, THD, is defined as

$$\mathrm{THD} = \frac{\sqrt{\sum_{n=2}^{\infty} I_h^2}}{I_1}, \tag{14}$$

where I_h is the harmonic current component of rank h and I_1 is the fundamental current component.

2.2.2 Fuzzy logic controller

Among the various available power filter controllers, such as IP, RST, hysteresis, and adaptive control, the fuzzy logic controller, which is used to design controllers with complex dynamics, has been tested on APF. In our application, the fuzzy control algorithm is implemented to control the DC side capacitor voltage based on processing of the DC voltage error $e(t)$ and its variation $\Delta e(t)$ in order to improve the dynamic of APF and reduce the total harmonic ratio of the source current.

The input variables are given by

$$\begin{aligned} e(t) &= V_c^{*2} - V_c^2, \\ \Delta e(t) &= e(t) - e(t-1). \end{aligned} \tag{15}$$

A fuzzy controller consists of fourth stages: fuzzification, knowledge base, fuzzification, inference mechanisms, and defuzzification. The knowledge base is composed of a data base and rule base, and is designed to obtain good dynamic response under uncertainty in process parameters and external disturbances. The data base, consisting of input and output membership functions, provides information for the appropriate fuzzification operations, the inference mechanism, and defuzzification. The inference mechanism uses a collection of linguistic rules to convert the input conditions into a fuzzified output. Finally, defuzzification is used to convert the fuzzy outputs into control signals.

Fig. 4 shows a block diagram of the proposed fuzzy logic control of the shunt active power filter.

The determination of the membership functions depends on the designer's experiences and expert knowledge. It is not easy to choose a particular shape that is better than others. A triangular membership function has the advantages of simplicity and easy implementation, and is adopted in this application [14, 15]. Fig. 5 shows the membership functions of the input and output linguistic variables.

In the design of a fuzzy control system, the formulation of its rule set plays a key role in improvement of the system performance. The rule table contains 49 rules as shown in Table 1, where (LP, MP, …) are linguistic codes (LP: large positive; MP: medium positive; SP: small positive; ZE: zero; LN: large negative; MN: medium negative; SN: small negative).

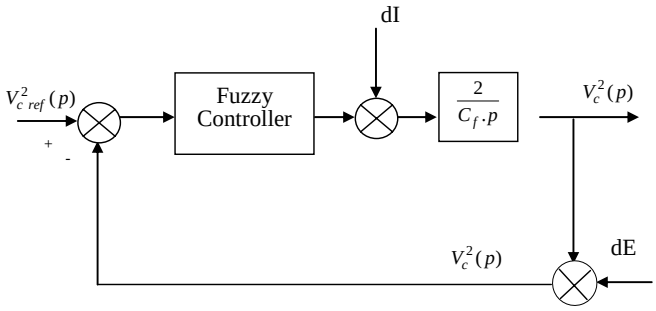

Fig. 4. Block diagram of the DC voltage control using a fuzzy controller.

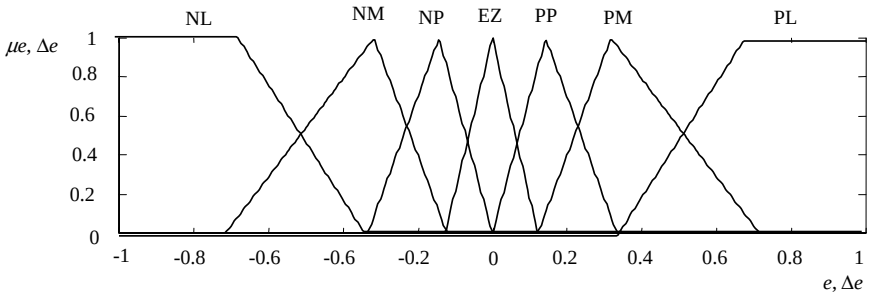

Fig. 5. Membership functions for the input variables (e, Δe) and output variable.

Table 1. Fuzzy control rule table.

Δe \ e	NL	NM	NS	EZ	PS	PM	PL
NL	NL	NL	NL	NL	NM	NS	EZ
NM	NL	NL	NL	NM	NS	EZ	PS
NS	NL	NL	NM	NS	EZ	PS	PM
EZ	NL	NM	NS	EZ	PS	PM	PL
PS	NM	NS	EZ	PS	PM	PL	PL
PM	NS	EZ	PS	PM	PL	PL	PL
PL	NL	NM	NS	EZ	PS	PM	PL

Various inference mechanisms have been developed to deffuzzify fuzzy rules. In this paper, we apply the max-min inference method to get an implied fuzzy set of turning rules [16, 17]. The imprecise fuzzy control action generated by the inference engine must be transformed into a precise control action in a real application. The center of mass method is used to deffuzzify the implied fuzzy control variables.

3. FUZZY HYSTERESIS BAND CURRENT CONTROL

To compensate the harmonics and fundamental reactive power, two current control methods can be considered, according to whether the regulated variables are line currents (i_s) or active power filter currents (i_f). Both methods are equivalent. In fact, the error signal at the input of the current regulator has the same dynamic; and only its sign is modified ($e = i_{fj}^* - i_{fj} = i_{sj} - i_{sj}^*$, $j = 1,\ 2,\ 3$). Our algorithm focuses on calculating and directly controlling the mains currents. The objective is to get the sinusoidal line currents in phase with the supply voltages at the common coupling point.

The commonly used current control strategies are the hysteresis current control, the ramp comparison control methods (natural, asymmetrical or optimal PWM) associated with linear controllers, and the predicted current control [10, 11]. The first method is very simple and easy to implement, but has the disadvantage of an uncontrollable high switching frequency. This high frequency places great stress on the power transistors and induces significant switching losses. The second and third methods allow operation at a fixed switching frequency and are usually performed using software with the system parameters. In this case, the operating conditions must be known to achieve sufficient, accurate control. Consequently, a fuzzy hysteresis band circuit control for a sinusoidal input current is applied in our application [17, 18].

An adaptive hysteresis band current control PWM technique can be programmed as a function of the active filter and supply parameters to minimize the influence of current distortions on the modulated waveform.

The width of the hysteresis band (HB) can be modulated at different points of the fundamental frequency of the cycle to control the PWM switching pattern of the inverter [13]. For symmetrical operation of all three phases, the band profiles, HB1, HB2, and HB3, should be same, but the phase will be displaced. The hysteresis band is given by

$$HB_j = \frac{V_c}{6.f_m.L_f}\ (1 - \frac{9L_f^2}{V_c}(\frac{v_{sj}(t)}{L_f} + \frac{di_{sj2}^*}{dt}),\ j = 1,\ 2,\ 3, \tag{16}$$

where f_m is the modulation frequency, i_s^* is the source reference current, di_s^*/dt represents its slope, L_f is the decoupling inductance of the APF, and V_c is the DC bus voltage.

Fig. 6 shows a block diagram of the adaptive hysteresis band current control using Eq. (16).

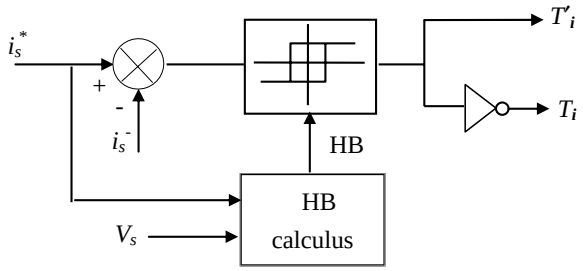

Fig. 6. Simplified model of an adaptive or fuzzy hysteresis-band current control.

To improve the active filter performance without precise knowledge of the APF parameters, the hysteresis band value can be implemented with a fuzzy logic controller. In this case, the supply voltage wave, $v_s(t)$, and main current reference slope, di_s^*/dt, can be selected as input variables to the fuzzy controller, and the hysteresis band hysteresis band magnitude (HB) as an output variable. The following step is used to determine the set of linguistic values associated with each variable. Each input variable is transformed into a linguistic size with five fuzzy subsets: PL is positive large, PM is positive medium, PS is positive small, EZ is zero, NL is negative large, NM is negative medium, and NS is negative small; for the output variable, HB, PVS is positive very small, PS is positive small, PM is medium positive, PL is positive large, and PVL is positive very large. The membership functions of the input and output variables are shown in Fig. 7, and the resulting inference rules are listed in Table 2.

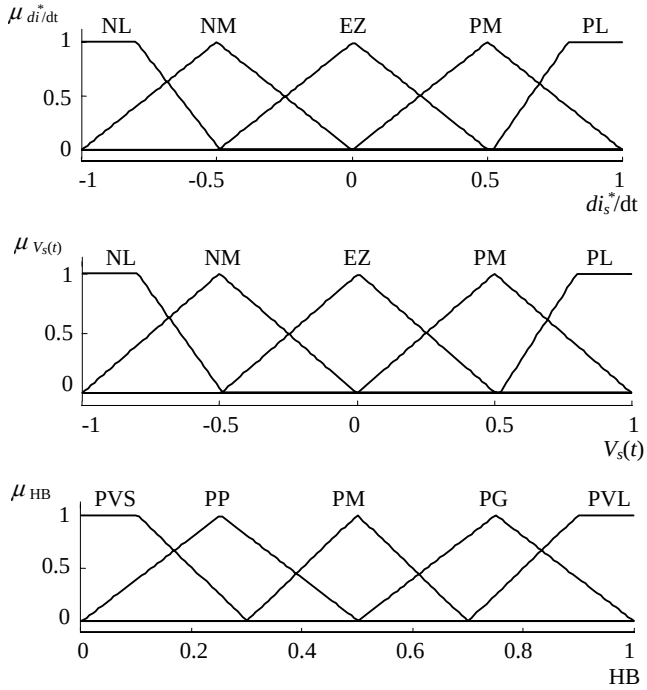

Fig. 7. Membership functions for the input variables di_s^*/dt and $V_s(t)$, and output variable HB.

4. SIMULATION RESULTS

The shunt active power was simulated using a model built in the Simulink environment of Matlab. The parameters of the system are as follows:

V_s = 220V rms, f_s = 50Hz, L_s = 15μH, L_f = 150μH, C_f = 1mF, and V_c = 700V.

The modulation frequency is fixed at 8 kHz.

Table 2. Resulting inference rules.

$V_s(t)$ \ di_{s1}^*/dt	NL	NM	EZ	PM	PL
NL	PL	PM	PM	PM	PL
NM	PL	PM	PS	PM	PL
EZ	PVL	PM	PVS	PM	PVL
PM	PL	PMM	PS	PM	PL
PL	PL	PM	PM	PM	PL

4.1 Optimization of the APF Parameters

Fig. 8 illustrates the performance of the PI voltage regulator for different cut off frequencies, f_c, under sudden change of the non linear load current. Results show that if the cut off frequency, f_c, increases, the variation, ΔV_c, of the DC supply voltage across the capacitor increases. This variation affects the filter current ripples and degrades the source current, THD. This investigation confirms that a trade off must be found between limiting the DC voltage fluctuation and the main current THD or reducing the voltage variation, ΔV_c, and settling time.

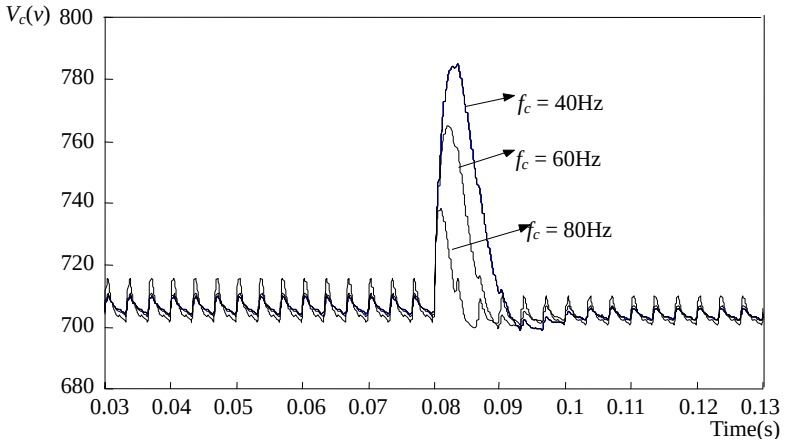

Fig. 8. DC voltage variation under load step changes for different cut off frequencies.

Figs. 9 (a) and (b) show the DC supply voltage variation during transient state using, respectively, a PI voltage regulator and a fuzzy controller for different values of the DC supply capacitor, C_f. If the capacitance value is reduced, the DC voltage fluctuation decreases but the DC voltage variation increases during a sudden change of the load current. However, when a PI voltage controller is used, we notice that a variation, ΔV_c, of 17% of the DC supply voltage is obtained, but that with a fuzzy logic voltage controller, a maximum change of the DC supply voltage of 5% is obtained. In other terms, for the

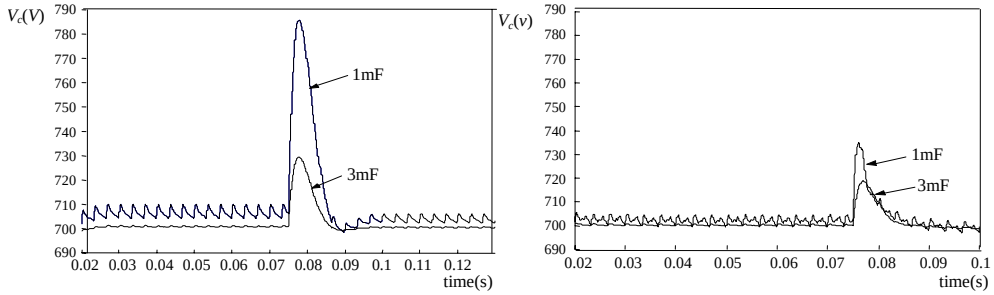

(a) (b)

Fig. 9. DC supply voltage variations under load step changes (a) with a PI regulator and f_c = 50Hz, and (b) with a fuzzy controller.

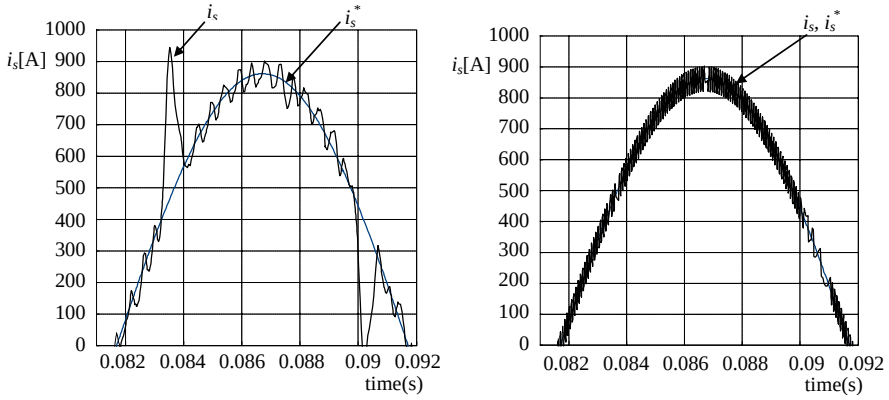

L_f = 450μH, THD = 15% L_f = 50μH, THD = 2.9%

Fig. 10. Half cycle waveforms of the source current and its reference in the case of a fixed hystersis band control.

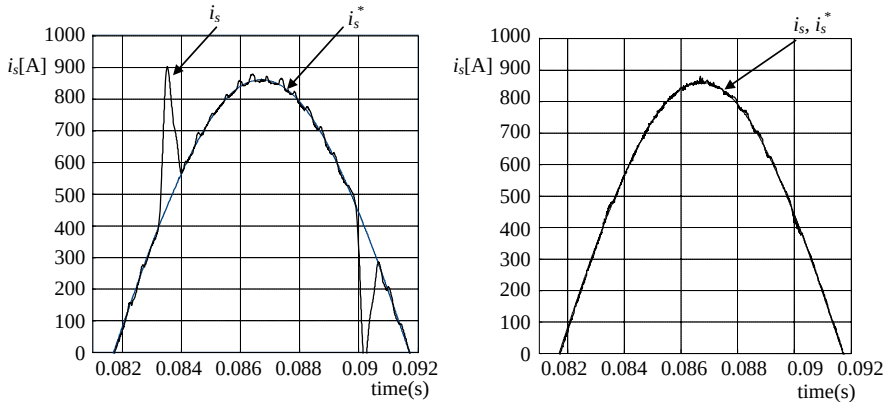

L_f = 450μH, THD = 15% L_f = 50μH, THD = 2.9%

Fig. 11. Half cycle waveforms of source current and its reference case of a fuzzy hysteresis band control.

same performance, we can considerably reduce the capacity value and its cost by using an appropriate robust fuzzy hysteresis controller without debasing the quality of the mains current following compensation. In this way, the capacitor value can be optimized.

Figs. 10 and 11 show waveforms of the source current, i_s, and its reference, i_s^*, on a half cycle when a hysteresis or a fuzzy hysteresis source courant controller is used.

Simulation results show that with a fixed hysteresis band control, the decrease of the decoupling inductance, L_f, value involves excessive ripple in the source current due to fast switching commutation of the APF but improves the source current THD.

The source current THD decreases from 29.5% to 15% in the case of a fixed hysteresis band for a change of the decoupling inductance from 450μH to 50μH. However, for fuzzy hysteresis source courant control, the variation of the decoupling inductance value does not greatly influence the source current ripples, and the variation of its value does not affect the fuzzy hysteresis band or the commutation frequency, which stays nearly constant. The source current THD decreases from 13% with L_f = 450μH to 1.47% with L_f = 50μH. Hence, we can choose a decoupling inductance with a reasonably low value such that the controllability of the output active filter is ensured with very weak ripples and a better THD of the source current.

The current error $\delta(t)$ between the source current is and its reference, i_s^*, was estimated in terms of the rms value. It should be noted that both controls, the hysteresis fixed band control and the fuzzy hysteresis band control, are able to follow the reference current, but that a performance difference consists in the ability to maintain a constant switching frequency and to limit ripples and peak currents with fuzzy controllers.

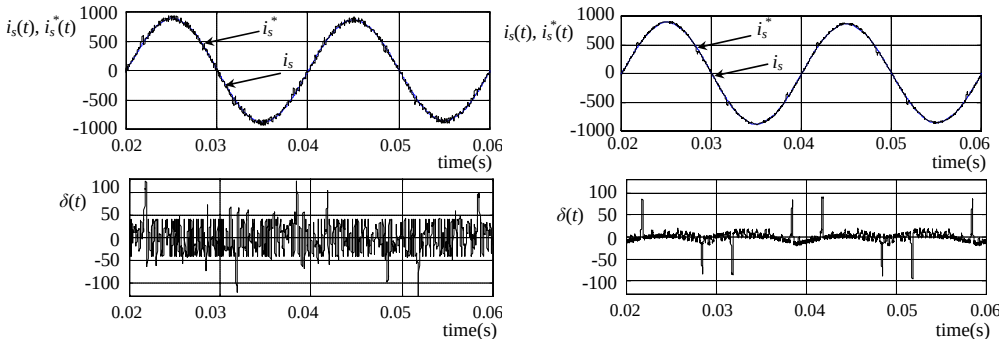

Fig. 12. Source current and current error $\delta(t)$ (a) with fixed hysteresis band control and (b) with a fuzzy hysteresis band control.

Simulation results shown in Figs. 12 (a) and (b) reveal, respectively, the current error, $\delta(t)$, in the case of a fixed or fuzzy hysteresis band control. Current peaks are more important than those produced by adaptive or fuzzy band controls, and the switching frequency changes many times per cycle. As a result, the switching losses are increased, and current source contains excessive harmonics.

When the current is controlled by means of a fuzzy hysteresis band as shown in Fig. 12 (b), the switching frequency is kept constant, and the current error is appreciably reduced, ensuring better global stability and insensitivity to parameter variation.

4.2 APF Steady-state and Transient Performances

Figs. 13 (a) and (b) show simulation results obtained with the studied system using the previously described current control techniques, i.e., the hysteresis and fuzzy logic controls.

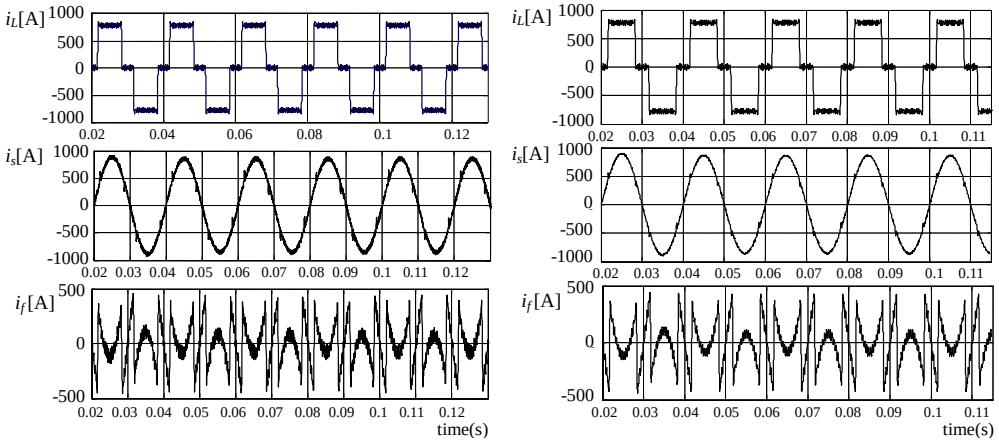

Fig. 13. Harmonic compensation (a) with a fixed hysteresis band control and (b) with a fuzzy hysteresis band control.

Fig. 13 shows the results of system operation with the fixed hysteresis band current control, where HB = 40A and the non linear load is a converter with a delay angle $\alpha = 0°$. This figure shows waveforms of the load current, active filter current, and source current. It shows that the source harmonic current is highly reduced, and that the THD of the mains current is decreased from 29.5% to 3.7%.

With a fuzzy hysteresis current controller, the system was simulated with the same parameters, and the modulation frequency was held nearly constant at 8KHz with HB_{max} = 40A. The performance of the proposed control algorithm of the active power filter is found to be excellent, and the source current is practically sinusoidal. The THD decreases from 29.5% before filtering to 2% with a fuzzy band after filtering as shown in Fig. 13 (b).

Fig. 14 shows the performance characteristics of the active power filter with the fuzzy control scheme, illustrating the steady state and transient behavior of the system. The simulation was conducted with a triggering delay angle $\alpha = 30°$ for a non linear load and a sudden load change at t = 63ms. Load and source currents, the active power filter current, and the DC capacitor voltage are shown. When the load increases, the source

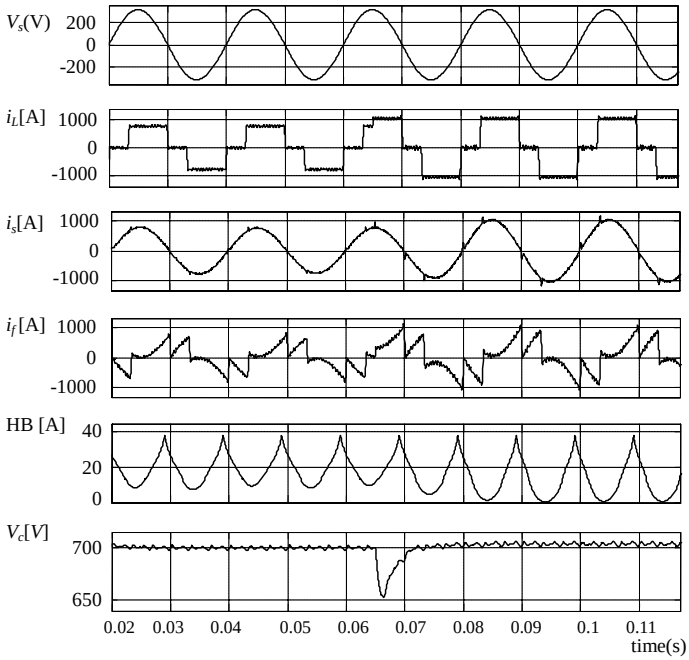

Fig. 14. Transient performance of the APF with fuzzy logic controllers.

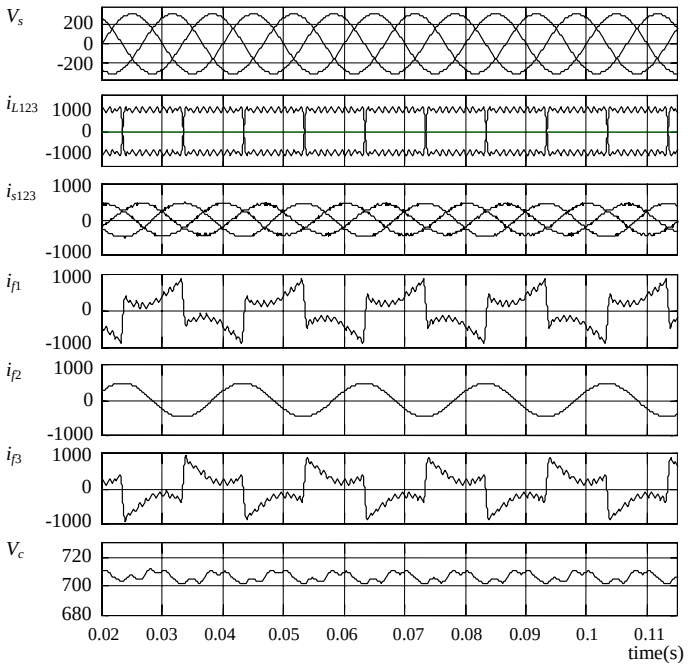

Fig. 15. Active power filter steady-state performance for harmonic and unbalanced current compensation (α = 30°).

currents respond very quickly and settle to steady state values within one cycle. The active power filter current increases almost instantaneously to meet the increased load current demand by taking the energy instantaneously from the DC capacitor. The DC voltage capacitor recovers within a cycle. The active power filter meets the requirements of harmonic and reactive components of the load current and keeps the source current sinusoidal under transient and steady state conditions and in phase with the source voltage.

Fig. 15 shows the system performance under an unbalanced nonlinear load, such as a single phase rectifier connected between two phases, 1 and 3. The active power filter acts only on the unbalanced load currents, compensates the source currents, and maintains the positive sequence first harmonic current system.

5. CONCLUSIONS

This paper has validated a simple control approach with a parallel active power filter based on the method of instantaneous real and imaginary powers used to identify the reference currents. Simulations results show the need for regulation of the DC voltage of the active filter and control of the current at its exit point. Two DC capacitor voltage controllers have been applied to improve the active power filter performance and simplify the design of the energy storage capacitor. The conventional fixed hysteresis band current control achieves fast response but generates excessive current ripples because the modulation frequency varies within one band. With the fuzzy hysteresis current control method, the band can be easily implemented with fuzzy logic to keep the modulation frequency nearly constant and to achieve good quality filtering. Application of fuzzy logic in the control loops enables us to choose optimal values of the inductance of decoupling and the storage capacity. With these types of controls, the active filter can be adapted easily to other more severe constraints, such as unbalanced conditions.

REFERENCES

1. H. Akagi, “New trends in active filters for power conditioning,” *IEEE Transactions on Industry Applications*, Vol. 32, 1996, pp. 1312-1322.
2. T. Thomas, K. Haddad, G. Joos, and A. Jaafari, “Design and performance of active power filters,” *IEEE Industry Applications Magazine*, Vol. 4, 1998, pp. 38-46.
3. M. Machmoum, N. Bruyant, M. A. E. Alali, and S. Saadate, “Compensateur actif série d’harmoniqes, de déséquilibre et de creux de tension des réseaux électrique,” *Revue Internationale de Génie Electrique*, Vol. 4, 2001, pp. 317-332.
4. H. Fujita, H. Akagi, and M. A. E. Alali, “The unified power quality conditioner: the integration of series-and shunt-active filter,” *IEEE Transactions on Power Electronics*, Vol. 13, 1998, pp. 315-322.
5. B. R. Lin, S. C. Tsay, and M. S. Liao, “Integrated power quality compensator based on sliding mode converter,” in *Proceedings of the European Conference on Power Electronics and Applications* (*EPE*), 2001.
6. N. Bruyant, M. Machmoum, and P. Chevrel, “Control of a three-phase active power filter with optimised design of the energy storage capacitor,” in *Proceedings of the*

IEEE Power Electronics Specialists Conference (*PESC*), Vol. 1, 1998, pp. 878-883.

7. M. Machmoum and N. Bruyant, "DSP based control of shunt active power filters for global or selective harmonics compensation," in *Proceedings of the International Conference on Harmonics and Quality of Power* (*ICHQP*), Vol. 2, 2000, pp. 661-667.
8. J. C. Le Bunetel and M. Machmoum, "Control of boost unity power factor correction systems," in *Proceedings of the IEEE Industrial Electronics Conference* (*IECON '99*), Vol. 1, 1999, pp. 266-271.
9. E. H. Watanabe, R. M. Stephan, and M. Aredes, "New concept of instantaneous active and reactive powers in electrical systems with generic loads," *IEEE Transactions on Power Delivery*, Vol. 8, 1993, pp. 697-703.
10. M. T. Tsai and W. I. Tsai, "Analysis and design of three-phase AC-to-DC converters with high power factor and near-optimum feed forward," *IEEE Transactions on Industrial Electronics*, Vol. 46, 1999, pp. 535-543.
11. J. C. Le Claire, S. Siala, J. Saillard, and R. Le Doeuff, "Novel analog modulator for PWM control of alternative currents," *Revue Internationale de Génie Electrique*, Vol. 3, 2000, pp. 109-131.
12. M. A. E. Alali, S. Saadate, Y. A. Chapuis, and F. Braun, "Energetic study of a shunt active conditioner compensating current harmonics, power factor and unbalanced," in *Proceedings of the International Conference on Power Electronics and Motion Control* (*EPE-PEMC*), Vol. 4, 2000, pp. 211-216.
13. B. K. Bose, "An adaptive hysteresis-band current control technique of a voltage fed PWM inverter for machine drive system," *IEEE Transactions on Industrial Electronics*, Vol. 37, 1990, pp. 402-408.
14. S. S. Min, K. C. Lee, J. W. Song, and K. B. Cho, "A Fuzzy current controller for field-orientated controlled induction machine by fuzzy rule," in *Proceedings of the IEEE Power Electronics Specialists Conference* (*PESC*), 1992, pp. 265-270.
15. J. M. Mendel, "Fuzzy logic systems for engineering: a tutorial," in *Proceedings of the IEEE*, Vol. 83, 1995, pp. 345-375.
16. H. Henao, G. A. Capolino, and J. A. Martinez-Velasco, "A new structure of fuzzy-hysteresis current controller for vector controlled induction machine drives," in *Proceedings of the IEEE Power Electronics Specialist Conference* (*PESC*), 1996, pp. 708-712.
17. M. Kale and E. Ozdemir, "A novel adaptive hysteresis band current controller for shunt active power filter," in *Proceedings of the IEEE Conference on Control Applications*, Vol. 2, 2003, pp. 1118-1123.
18. S. Jain, P. Agrawal, and H. Gupta, "Fuzzy logic controlled shunt active power filter for power quality improvement," in *IEE Proceedings of the Electric Power Applications*, Vol. 149, 2002, pp. 317-28.

Benyounès Mazari (1953) received the state engineer degree in Electrical Engineering in 1978 from the University of Sciences and Technology of Oran (USTO) Algeria, the M.S. degree from the University of Colorado Boulder U.S.A. in 1981 and the doctorat degree from the Institut National Polytechnique de Lorraine (INPL) Nancy France in 1992. Since 1982, he was at the USTO-Oran and from 1987-1992 he was on leave as a researcher at INPL (France). Since 1992 he was a Professor of Electrical Sciences at the same university. His area of research includes power electronics, traction drives, and harmonics in power systems.

Fatiha Mekri was born in Algeria 1970. She received the Diplo. Ing. and the M.S. degrees in Electrical Engineering from the University of Sciences and Technology of Oran, Algeria respectively in 1994 and 2001. She is currently working toward the doctorat degree. Her area of interest are active power filters, applications of power electronics, and control techniques.